ELSEVIER

Journal of Molecular Catalysis A: Chemical 160 (2000) 277–285

JOURNAL OF MOLECULAR CATALYSIS A: CHEMICAL

www.elsevier.com/locate/molcata

Nafion–RuO_2–$Ru(bpy)_3^{2+}$ composite electrodes for efficient electrocatalytic water oxidation

K. Chandrasekara Pillai [a,*], A. Senthil Kumar [a], Jyh-Myng Zen [b]

[a] *Department of Physical Chemistry, University of Madras, Guindy Campus, Madras, 600 025, India*
[b] *Department of Chemistry, National Chung-Hsing University, Taichung 402, Taiwan*

Received 5 January 2000; accepted 1 May 2000

Abstract

Electrocatalytic water oxidation to evolve O_2 was studied on a Nafion–RuO_2–$Ru(bpy)_3^{2+}$ composite electrode. The O_2 evolution current efficiency was largely improved for the multi-component electrode over the Nafion–RuO_2 and Nafion–$Ru(bpy)_3^{2+}$ individuals. The redox mediation through the $Ru(bpy)_3^{2+}$ was found to dominate over the RuO_2 catalytic effect in the water oxidation mechanism. The specific surface area of the RuO_2, which was prepared at different temperatures (300–700°C), used in fabricating the composite electrode also played an important role in the overall water oxidation mechanism. Both the reaction and electrode parameters were optimized to get effective electrocatalytic current values in this study.

Keywords: Electrocatalysis; Water oxidation; Nafion; RuO_2; $Ru(bpy)_3^{2+}$

1. Introduction

Water oxidation has been the focus of intensive study due to its importance in photosynthesis, and in designing artificial photosynthetic system for solar energy conversion to obtain a renewable energy resource [1–8]. Unfortunately, the high overpotential for the $4e^-$ oxidation of H_2O to O_2 makes the process less feasible. One way to improve this is to use suitable oxygen evolution catalysts (Cat_{OER}), like RuO_2, IrO_2, PtO_2, etc., together with photosensitizers (PSn), such as $Ru(bpy)_3^{2+}$, $Fe(bpy)_3^{2+}$, $Fe(phen)_3^{2+}$, etc. On the other hand, various molecular-based catalysts, such as oxo-bridged ruthenium dimers ($[L_2(H_2O)Ru–O–Ru(H_2O)L_2]^{4+}$, where L = 2,2′-bipyridine and 4,4′-dichloro or 5,5′-dichloro-2,2′-bipyridine [5, 9–12]), in combination with suitable oxidants, like Ce^{4+}, MnO_4^-, IO_4^-, PbO_2, BrO_3^-, $Ru(bpy)_3^{3+}$, $Fe(bpy)_3^{3+}$ were also reported for this purpose [13]. The chief advantage in using the integrated Cat_{OER}/PSn system, however, is that the Cat_{OER} contains specific higher oxidation redox groups (e.g., Ru(VII)/Ru(VI) and Ru(VI)/Ru(IV) for RuO_2) and surface area, which cannot be expected in the simple molecular-based catalyst systems [8]. Majority of work shows that the catalyst RuO_2 and the photosen-

* Corresponding author. Fax: +91-44-2352870.
E-mail address: kchandra@unimad.ernet.in (K.C. Pillai).

1381-1169/00/$ - see front matter
PII: S1381-1169(00)00262-4

sitizer $Ru(bpy)_3^{2+}$ are the best combination for H_2O decomposition, in which $Ru(bpy)_3^{3+}$, formed from the electronically excited complex $[Ru(bpy)_3^{2+}]^*$, serves as the oxidant [1–3,8,13]. Although the photochemical aspects in combining RuO_2 with $Ru(bpy)_3^{2+}$ were thoroughly studied, surprisingly, very little attention was paid to its electrochemical aspects. The interaction of the catalyst RuO_2 with the oxidant $Ru(bpy)_3^{3+}$ (i.e., the dark process in the photochemical reaction) was especially ignored, which is one of the key processes in the overall H_2O oxidation step [13]. To investigate these aspects, in this work, electrochemical techniques were used to generate the oxidant $Ru(bpy)_3^{3+}$ and to study the oxygen evolution efficiencies.

The combination of Cat_{OER} with PSn in a compact, multi-layer polymer matrix can effectively solve the experimental difficulties faced in solution phase homogeneous and heterogeneous photocatalytic systems. In the present investigation, recast Nafion films were used as the polymer matrix to achieve efficient water oxidation. As to our knowledge, no such studies were undertaken before. In the present work, a systematic investigation was made to prepare the Nafion (0.1–1%)–RuO_2 (0.03%)–$Ru(bpy)_3^{2+}$ composite electrodes to achieve the maximum oxygen evolution efficiency. The experimental parameters, including the RuO_2 preparation temperature (a key factor to achieve different surface area, particle size, and porosity [14]), RuO_2 loading amount, Nafion composition, solution pH, and operating potential were thoroughly studied.

2. Experimental

2.1. Materials and catalyst preparation

Nafion 117 solution (5% w/v solution in a mixture of lower aliphatic alcohols) obtained from Aldrich Chemical was used to prepare required dilutions by freshly distilled ethanol. $RuCl_3 \cdot xH_2O$ was purchased from Arora Matthey, India and used without further purification. The complex $Ru(bpy)_3^{2+}$ was prepared according to the procedure reported in the literature [15], and its formation was confirmed by UV–visible spectroscopy (peak at 452 nm). All the other chemicals used were of reagent grade. RuO_2 powders were prepared from $RuCl_3 \cdot xH_2O$ by high temperature pyrolyzing technique [16]. In brief, $RuCl_3 \cdot xH_2O$ (3 g) was first dried at 100°C for 1 h, crushed in agate mortar in hot condition, transferred to a quartz silica boat and placed in muffle furnace, which was kept preheated at 150°C. Furnace temperature was then varied gradually to the preset preparation temperature of 300–700°C for the formation of RuO_2 crystallites, and the samples were heated in the presence of O_2 stream at a pressure of 20–30 $dm^3\ h^{-1}$ for 6 h. The samples were taken out, crushed again, and finally heated at the same temperature for another 6 h. Furnace temperatures were initially standardized with the help of a standard Chromel–Alumel thermocouple using standard EMF values [17]. The catalyst powders were thoroughly washed in double distilled water until the solution gave a negative test for Cl^- with Ag^+, and finally dried at 110°C for 12 h. BET surface area measurements were performed using Carlo Erba Strumentazione Microstructure Lab instrument using N_2 gas adsorption technique.

2.2. Apparatus

Cyclic voltammetry was conducted with a Wenking Potentiostat (Model ST 72), a Wenking scan generator (Model VSG 83) and a Graphtec XY recorder (Model WX 2300). A conventional H-type cell, equipped with a large area platinum plate as a counter electrode and a saturated calomel electrode (SCE) with lugging capillary as a reference electrode, was employed throughout the studies. N_2 gas was used for deaerating the experimental solution.

2.3. Preparation of the Nafion-modified electrodes

To prepare the Nafion-coated glassy carbon electrode (Nafion-GCE), 7 μl of the Nafion solution of desired weight percentage (0.1–1% w/v) was coated onto the pretreated GCE (geometrical area of 0.0707 cm^2) followed by air-drying for 25–30 min. The GCE was initially abraded with increasingly fine grades of emery paper down to mirror finish, degreased with trichloroethylene, washed with copious amount of double distilled water, followed by potential cycling for four times in the deaerated base electrolyte in the potential region 0.0 to 1.4 V (RHE) at a potential scan rate (υ) = 20 mV s^{-1}. As for the Nafion–$Ru(bpy)_3^{2+}$ electrode, the Nafion-GCE was dipped in 1 mM $Ru(bpy)_3^{2+}$ in 0.1 M H_2SO_4 or pH 4.6 of acetate buffer solution for 10–15 min, removed, washed thoroughly with double distilled water, and cycled between 0.45 and 1.15 V (RHE) in the supporting electrolyte until the voltammetric peaks became constant. For preparing the Nafion–RuO_2 electrode, the diluted Nafion solution containing RuO_2 suspensions (0.03% w/v) was sonicated for 5–10 min until the suspensions became fully dispersed, and the clear colloidal solution was then coated on to the pretreated GCE and dried. Finally, the Nafion–RuO_2–$Ru(bpy)_3^{2+}$ composite electrode was prepared by loading $Ru(bpy)_3^{3+}$ into the Nafion–RuO_2 electrode, following the procedure described above for the Nafion–$Ru(bpy)_3^{2+}$ electrode.

3. Results and discussion

Fig. 1 shows the typical cyclic voltammetric responses of the Nafion-modified electrodes recorded at 20 mV s^{-1} scan rate in 0.1 M H_2SO_4 acid solution. It is clear that no specific redox peaks were noticed for both the Nafion-GCE (curve a) and the Nafion–RuO_2 electrode (curve b). On the other hand, a well-defined pair of redox peaks with the formal potential, $E^{0\prime}$, 1.02 V (SCE) corresponding to the oxidation and reduction of $Ru(bpy)_3^{3+/2+}$ was observed with the Nafion–$Ru(bpy)_3^{2+}$ electrode (curve a′). The same redox process was observed with

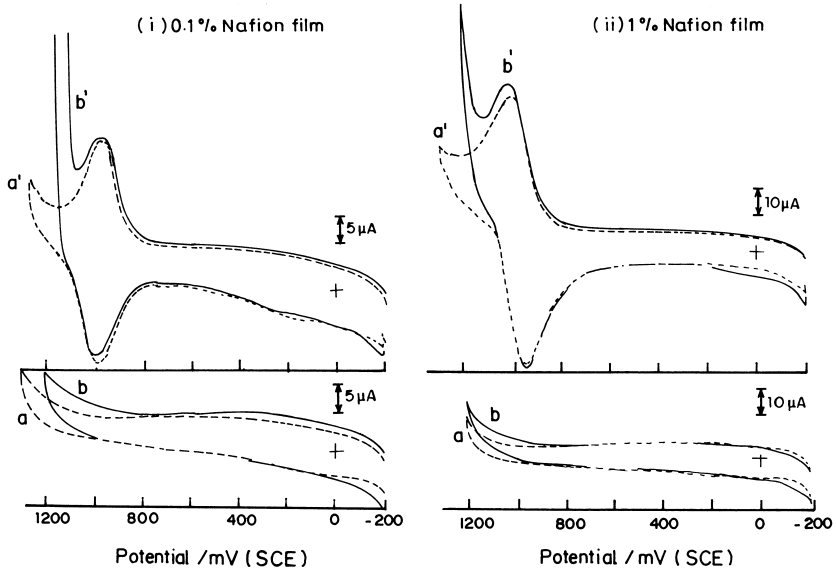

Fig. 1. Cyclic voltammetric responses of Nafion-modified electrodes in 0.1 M H_2SO_4 solution at υ = 20 mV s^{-1}: (i) 0.1% Nafion film; (ii) 1% Nafion film: (a) Nafion-GCE; (b) Nafion–RuO_2 (0.03%, 700°C) electrode; (a′) Nafion–$Ru(bpy)_3^{2+}$ electrode; (b′) Nafion–RuO_2 (0.03%, 700°C)–$Ru(bpy)_3^{2+}$ electrode.

the Nafion–RuO_2–$Ru(bpy)_3^{2+}$ electrode (curve b′), which also showed a greatly enhanced oxygen evolution current. Note that the redox peaks of $Ru(bpy)_3^{2+/3+}$ were not affected by the presence of RuO_2 in the film. Most important of all, the appearance of the cathodic peak in the reverse scan (curve b′) indicated that there was no mediated H_2O oxidation by the electrogenerated $Ru(bpy)_3^{3+}$ in the presence of RuO_2 in 0.1 M H_2SO_4.

The performance of the Nafion-modified electrodes was also studied in pH 4.6 acetate buffer and the voltammograms are presented in Fig. 2. Interestingly, compared to Fig. 1, the cathodic peak in Fig. 2 showed a decreased intensity, suggesting that the $Ru(bpy)_3^{3+}$ formed at the anodic peak was removed by H_2O through a chemical reaction. It is therefore clear that the O_2 evolution reaction was mediated by the electrogenerated $Ru(bpy)_3^{3+}$ complex and catalyzed by the RuO_2 dispersions in the Nafion film in pH 4.6 solution. The absence of the $Ru(bpy)_3^{3+}$-mediated catalysis in 0.1 M H_2SO_4 is understandable, since $E^{0\prime}$ at this pH for $Ru(bpy)_3^{3+/2+}$ and O_2/H_2O are 1.02 V (SCE) and 0.98 V

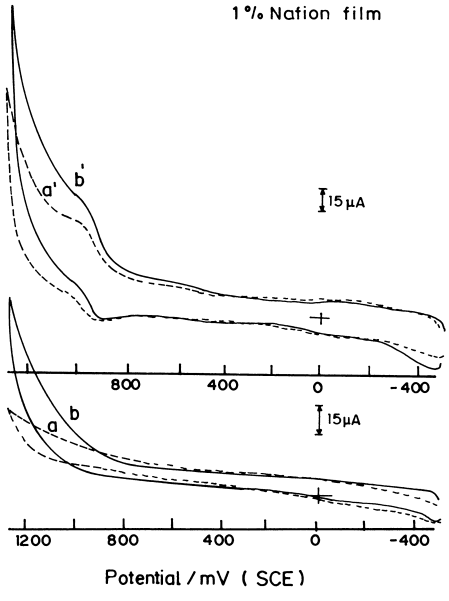

Fig. 2. Cyclic voltammetric responses of 1% Nafion film-modified electrodes in pH 4.6 acetate buffer solution at $v = 20$ mV s^{-1}. Other assignments are the same as in Fig. 1.

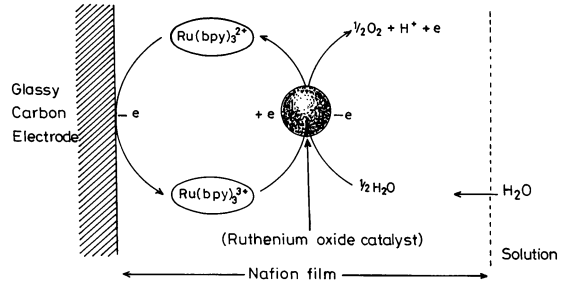

Fig. 3. Schematic representation of water oxidation reaction at the Nafion–RuO_2–$Ru(bpy)_3^{2+}$ multi-component electrode.

(SCE), respectively [8,13], so that $Ru(bpy)_3^{3+}$ cannot accept electron from H_2O. But in pH 4.6 acetate buffer the $E^{0\prime}$ of O_2/H_2O is 0.68 V (SCE), and therefore the thermodynamic driving force for the reaction is substantially greater (340 mV) than that in 0.1 M H_2SO_4. Fig. 3 illustrates the possible electrocatalytic H_2O oxidation reaction at the Nafion–RuO_2–$Ru(bpy)_3^{2+}$ composite electrode.

As shown in Fig. 2, the voltammograms of all the Nafion-modified electrodes showed a sharp increase in current signals at high anodic potentials due to the anodic oxidation of the solvent H_2O. This process, which started occurring at a potential ≈ 1.05 V (SCE) at the Nafion-GCE (curve a) and the Nafion–$Ru(bpy)_3^{2+}$ electrode (curve a′), was initiated at a less positive potential 0.9 V (SCE) at the Nafion–RuO_2 electrode (curve b). Moreover, the current increase at the Nafion–RuO_2 electrode was accompanied by a visible formation of tiny oxygen gas bubbles near the electrode surface especially at higher anodic potentials. This finding is in accordance with the previous reports by Shieh and Hwang [18], who also observed that the amount of O_2 gas collected at a PTFE-modified RuO_2 electrode in the anodic potential regions was in quantitative agreement with the oxygen-generated charge. Interestingly, compared to the Nafion–RuO_2 electrode, the Nafion–RuO_2–$Ru(bpy)_3^{2+}$ multi-component electrode showed a marked increase in both the anodic current signal and the oxygen gas bubble formation, at any given potential, as illustrated

by curve b′ of Fig. 2, thus confirming the RuO_2-catalyzed $Ru(bpy)_3^{3+}$-mediated oxygen gas evolution from water decomposition [2,3].

Note that in solution phase photochemical reactions involving multiple components in solution, the water oxidation to O_2 was not a straightforward process due to the occurrence of many unwanted side reactions. For example, RuO_2 catalyst was not specific towards water oxidation alone, and it was shown to promote hydrogen generation as well [19,20]. Besides, RuO_2 catalyst was found to aid the mediated oxidation of the protective agent, used to stabilize the catalyst particles, over that of water [21]. Moreover, mere reduction of Ru^{3+} complex to Ru^{2+} did not guarantee stoichiometric quantities of O_2 evolution; this was attributed to irreversible decomposition of Ru^{3+} complex occurring in competition with the water oxidation [22,23]. Precisely, for these reasons, in-situ physical methods like oxygen-sensing electrodes, gas chromatography, etc., were used in solution phase photochemical water oxidation studies to confirm the O_2 formation and measure the oxygen gas evolved. The above mentioned drawbacks associated with solution-phase water oxidation experiments could be traced back to the fact that in these systems catalytic sites in Cat_{OER} were not energetically fixed and always not close to make effective collision with PSn to generate the product, viz., O_2. As for the O_2 evolution at the positively polarized Nafion–RuO_2–$Ru(bpy)_3^{2+}$ electrode in the present study is considered, these problems may not arise for the following two reasons: (1) the applied positive electrical field ensured that PSn and Cat_{OER} sites in Nafion were energetically fixed to react favourably and produce oxygen; (2) Yagi et al. [24] showed that with the incorporation of Ru^{3+} complex catalyst into Nafion membrane, the amount of O_2 evolved and the catalyst activity were remarkably increased, compared to the homogeneous solution system. This was attributed to a decrease in the bimolecular decomposition of the Ru^{3+} catalyst in the polymer film. Basing on this, one could expect that the decomposition and the deactivation of $Ru(bpy)_3^{3+}$ complex and RuO_2 catalyst were suppressed by incorporating them into the Nafion film. In addition to this, because of the presence of both RuO_2 and $Ru(bpy)_3^{3+}$ together in the polymer matrix, their proximity could bring cooperative catalysis possible (vide infra), and their combination could lead to water decomposition reaction only, at the Nafion–RuO_2–$Ru(bpy)_3^{2+}$ electrode under the present experimental conditions as per the reaction scheme described in Fig. 3.

As the voltammogram at more positive potentials > 1.5 V (SCE) resulted in the rupture of the Nafion film due to vigorous bubble formation from the interstitial sites of the composite electrode, the voltammetric experiments with all the modified electrodes were restricted to a maximum anodic sweep potential of 1.3 V (SCE).

Trends similar to those in Figs. 1 and 2 were observed, with other Nafion electrodes fabricated using RuO_2 powders prepared at different temperatures (600–300°C).

In order to compare the catalytic efficiency of the modified electrodes, two parameters, E_{OER}, the potential at which oxygen evolution started, and, i_{OER}, the anodic oxygen evolution current measured at 1.30 V (SCE), were estimated from the above quasi steady-state cyclic voltammograms for the individual electrodes and the composite electrode. Typical data for thin (0.1% Nafion) and thick (1% Nafion) film electrodes are assembled in Tables 1 and 2, respectively. It is clear from the Tables that for both thin and thick film electrodes, the Nafion–RuO_2–$Ru(bpy)_3^{2+}$ composite electrode had more efficient water oxidation current than the individual electrodes, i.e., Nafion-GCE, Nafion–RuO_2, and Nafion–$Ru(bpy)_3^{2+}$ electrodes. A comparison of the performance shows that the Nafion (0.1%)–RuO_2–$Ru(bpy)_3^{2+}$ electrode had higher efficiency over the Nafion (1%)–RuO_2–$Ru(bpy)_3^{2+}$ electrode.

Experiments with different weight percentage of the Nafion coating resulted in the variation of

Table 1
Water oxidation potential (E^{a}_{OER}) and oxygen evolution current (i_{OER}) at 1.3 V[a] for the 0.1% Nafion film electrodes in pH 4.6 acetate buffer

T (°C)	(1) Nafion (0.1%)–GCE		(2) Nafion (0.1%)–RuO_2 (0.03%)		(3) Nafion (0.1%)–$Ru(bpy)_3^{2+}$		(4) Nafion (0.1%)–RuO_2 (0.03%)–$Ru(bpy)_3^{2+}$		Catalytic current (μA)[b]	
	E_{OER} (mV)	i_{OER} (μA)	E_{OER} (mV)	i_{OER} (μA)	E_{OER} (mV)	i_{OER} (μA)	E_{OER} (mV)	i^{c}_{OER} (μA)[c]	Due to RuO_2 alone [(2)–(1)]	Due to $Ru(bpy)_3^{2+}$ alone [(4)–(2)]
700	1040	26.5	920	73.5	1060	54.5	875	143.5	47.0	70.0
600	1040	26.5	920	91.5	1060	54.5	860	118.5	65.0	27.0
500	1040	26.5	900	96.8	1060	54.5	850	195.0	70.3	98.2
400	1040	26.5	920	160.5	1060	54.5	880	471.0	134.0	310.5
300	1040	26.5	920	442.5	1060	54.5	905	1710.0	416.0	1267.5

[a] Potentials are referred with respect to SCE.
[b] Individually contributed current to the overall catalytic current of the composite electrode (see text).
[c] Overall catalytic current of the composite electrode.

the following: (1) the film thickness, (2) the loading amount of $Ru(bpy)_3^{2+}$, and (3) the nature of the charge transport process within the film. While the film thickness of the Nafion coating depended directly on the coating weight of the polymer, it was not true for $Ru(bpy)_3^{2+}$ loading. The total surface concentration (Γ_T) of the $Ru(bpy)_3^{2+}$ complex in the Nafion film was calculated from the anodic charge (Q_a) under the voltammetric peak recorded at $\upsilon = 20$ mV s^{-1}, using the equation $Q_a = nFA\Gamma_T$ [25], where n is the number of electrons of the reaction, A the electrode geometric area, and F the Faraday constant. With $n = 1$, Γ_T was calculated to be 6.61×10^{-10} and 2.63×10^{-10} mol cm^{-2} in Nafion's 1% and 0.1% films, respectively. Note that the 10 times diluted solution of 1% Nafion yielded only 2.51 times decrease in the Γ_T value in the films, which was reminiscent of the relatively higher accumulation force of $Ru(bpy)_3^{2+}$ species per unit area of the 0.1% Nafion sites. Regarding the charge transport process, the logarithmic plots of the anodic peak current (i_{pa}) vs. scan rate from cyclic voltammograms of 0.1% and 1% Nafion–$Ru(bpy)_3^{2+}$ electrodes produced

Table 2
Water oxidation potential (E^{a}_{OER}) and oxygen evolution current (i_{OER}) at 1.3 V[a] for the 1% Nafion film electrodes in pH 4.6 acetate buffer

T (°C)	(1) Nafion (1%)–GCE		(2) Nafion (1%)–RuO_2(0.03%)		(3) Nafion (1%)–$Ru(bpy)_3^{2+}$		(4) Nafion (1%)–RuO_2 (0.03%)–$Ru(bpy)_3^{2+}$		Catalytic current (μA)[b]	
	E_{OER} (mV)	i_{OER} (μA)	E_{OER} (mV)	i_{OER} (μA)	E_{OER} (mV)	i_{OER} (μA)	E_{OER} (mV)	i_{OER} (μA)[c]	Due to RuO_2 alone [(2)–(1)]	Due to $Ru(bpy)_3^{2+}$ alone [(4)–(2)]
700	1090	31.5	900	113.3	1100	107.3	855	187.5	81.8	74.3
600	1090	31.5	920	47.3	1100	107.3	840	156.0	15.8	108.8
500	1090	31.5	905	111.8	1100	107.3	860	236.3	80.3	124.5
400	1090	31.5	900	127.5	1100	107.3	875	412.5	96.0	285.0
300	1090	31.5	910	485.0	1100	107.3	890	1120.0	453.5	635.0

[a] Potentials are referred with respect to SCE.
[b] Individually contributed current of the overall catalytic current of composite electrode (see text).
[c] Overall catalytic current of the composite electrode.

Table 3
BET surface area data of RuO_2 powders prepared at different temperatures

T (°C)	Specific surface area ($m^2\ g^{-1}$)	Pore specific volume ($10^3\ cm^3\ g^{-1}$)	Sample density ($g\ m^{-3}$)
700	14.49	6.15	1.01
600	24.68	9.55	1.02
500	20.67	8.54	0.90
400	27.30	10.79	0.94
300	52.40	21.29	0.82

$[\partial\log(i_{pa})/\partial\log(\upsilon)]$ values 0.91 and 0.45, suggesting thin layer behaviour in 0.1% Nafion film and semi-infinite behaviour in 1% Nafion film. Clearly, charge transport in 0.1% Nafion film was much faster than in 1% Nafion film [26]. In addition, we believe that in the 0.1% Nafion film, the PSn and Cat_{OER} were separated by very closer distances (since the employed amount of RuO_2 was constant, viz., 0.03% w/v both in 0.1% and 1% Nafion films), thus accompanied with lower energy barrier for the product formation.

The catalytic current of the Nafion–RuO_2–$Ru(bpy)_3^{2+}$ composite electrode was found to increase with decrease in the preparation temperature of the RuO_2 samples (see column 9 of Tables 1 and 2). Table 3 summarizes the BET surface area data of the RuO_2 powders prepared at different temperatures. The RuO_2 samples prepared at higher temperatures (i.e., 500–700°C) possessed lower specific surface area than the low temperature prepared ones (i.e., 300°C and 400°C). Thus, the catalytic reactivity of the composite electrodes towards H_2O oxidation was apparently governed by the specific surface area of the RuO_2.

The individual contribution by the component $Ru(bpy)_3^{2+}$ alone to the overall catalytic current of the Nafion–RuO_2–$Ru(bpy)_3^{2+}$ electrode was obtained by subtracting the i_{OER} of the Nafion–RuO_2 electrode from the i_{OER} of

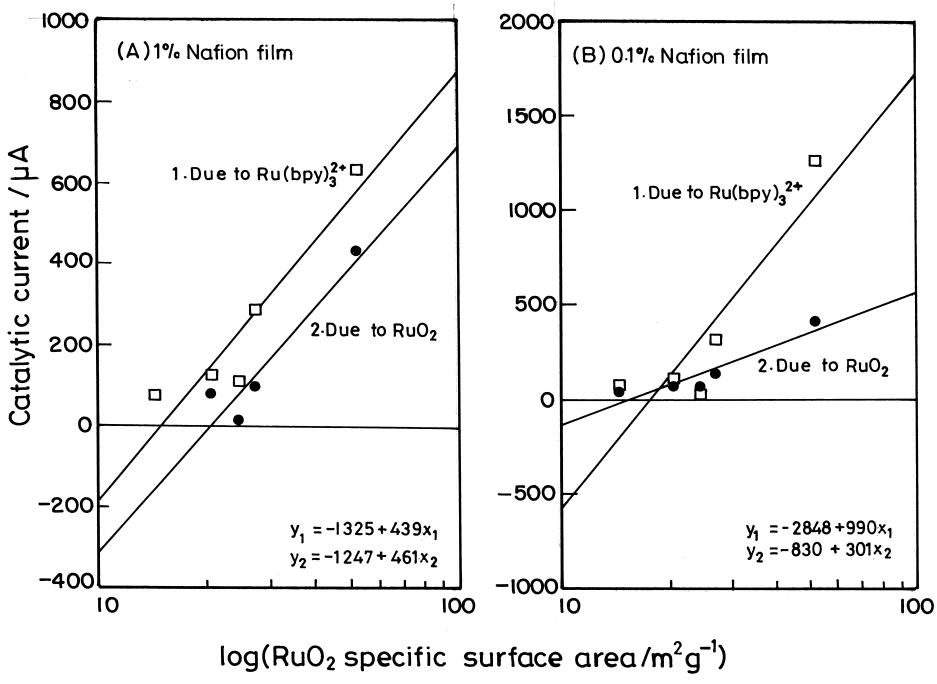

Fig. 4. Plot of catalytic current vs. log(RuO_2 specific surface area) for H_2O oxidation reaction in pH 4.6 acetate buffer solution: (A) Nafion (1%)–RuO_2 (0.03%)–$Ru(bpy)_3^{2+}$ electrode ; (B) Nafion (0.1%)–RuO_2 (0.03%)–$Ru(bpy)_3^{2+}$ electrode.

the multi-component electrode. As RuO_2 is intrinsically catalytic towards O_2 evolution, the i_{OER} of the Nafion–RuO_2 electrode less the i_{OER} of Nafion-GCE represents more appropriately its individual contribution to the overall catalytic current of the composite electrode. The values calculated for different temperature electrodes are listed in the penultimate columns of Tables 1 and 2. The effect of the specific surface area of RuO_2 on the individually contributed catalytic current, by RuO_2 alone and $Ru(bpy)_3^{2+}$ alone, is shown in Fig. 4A for 1% Nafion electrodes. Fig. 4B describes similar plots for 0.1% Nafion electrodes. Several points could be concluded from these plots: first, acceptable straight lines were observed verifying the surface area effect to the increase in catalytic current; second, the $Ru(bpy)_3^{2+}$ was seen to contribute more than the RuO_2 in the overall water oxidation reaction; third, the slopes obtained for the two curves in Fig. 4A were almost equal, revealing that in thick Nafion films the catalyst RuO_2 simply acted, with fixed catalytic sites per unit area, to effectively combine the H_2O and $Ru(bpy)_3^{3+}$ for higher catalytic efficiency. Fourth, the curves in Fig. 4B showed different trends, where ~ 3.5 times/decade of higher catalytic current was noticed for $Ru(bpy)_3^{2+}$ over the RuO_2 effect. This observation, coupled with the fact that the slope in Fig. 4B for RuO_2 is close to that in Fig. 4A, reveals that the H_2O oxidation reaction was greatly facilitated in the thin film multi-component electrode, due to certain additional process along with the catalyst surface area effect. A cooperative interaction between RuO_2 catalyst and the $Ru(bpy)_3^{2+}$ complex in the film can be envisaged to account for the improved O_2 evolution efficiency, and according to Fig. 4B, the interaction between the $CatO_2$ and PSn is a linear function of the RuO_2 surface area. This effect along with the facile electron transfer, and the closer proximity of the $CatO_2$ and PSn allowed the thin film composite electrode to function with a drastically enhanced catalytic activity compared to its thick film counterpart.

The optimized conditions for fabricating the Nafion (0.1%)–RuO_2–$Ru(bpy)_3^{2+}$ multi-component electrode were the following: (a) Nafion: 0.1%, (b) RuO_2 preparation temperature: 300°C, (c) RuO_2 loading amount: 0.03% w/v, (d) pH: 4.6 (acetate buffer/0.1 M). Since the thin film multi-component electrode is transparent and shows good stability, its integration with the cyclic photo-assisted water decomposition system may offer an easy route for solar energy conversion. In this context, the facility to bias the surface-bound multi-component polymer electrode may provide an additional advantage to the solar conversion process.

Acknowledgements

The authors gratefully acknowledge the financial support from the Council of Scientific and Industrial Research, New Delhi, India.

References

[1] J. Kiwi, M. Gratzel, Angew. Chem., Int. Ed. 18 (1979) 423.
[2] K. Kalyanasundram, O. Micic, E. Pramauro, M. Gratzel, Helv. Chim. Acta 62 (1979) 2432.
[3] M. Gratzel, in: M. Gratzel (Ed.), Energy Resource Through Photochemistry and Catalysis, Academic Press, New York, 1983.
[4] R.-J. Lin, M. Kaneko, in: K. Sienicki (Ed.), Molecular Electronic and Molecular Electronic Devices vol. 1 CRC Press, Tokyo, 1993, p. 207.
[5] K. Nagoshi, S. Yamashita, M. Yagi, M. Kaneko, J. Mol. Catal. A 144 (1999) 71.
[6] T. Abe, Y. Tamada, H. Shiroishi, M. Nukaga, M. Kaneko, J. Mol. Catal. A 144 (1999) 389.
[7] K.C. Pillai, A. Senthil Kumar, V. Dharuman, Bull. Electrochem. 12 (1996) 432.
[8] A. Senthil Kumar, PhD Dissertation, Department of Physical Chemistry, University of Madras, India, 1998.
[9] Y.-K. Lai, K.-Y. Wong, J. Electroanal. Chem. 380 (1995) 193.
[10] T.J. Meyer, J. Electrochem. Soc. 131 (1984) 221C.
[11] R. Ramaraj, A. Kira, M. Kaneko, J. Chem. Soc., Faraday Trans. 1 82 (1987) 1539.
[12] R. Ramaraj, A. Kira, M. Kaneko, Angew. Chem., Int. Ed. 25 (1986) 1009.
[13] A. Mills, Chem. Soc. Rev. 18 (1989) 285.
[14] A. Senthil Kumar, K.C. Pillai, J. Solid State Electrochem., in press.
[15] I. Fujita, Kobayashi, J. Chem. Phys. 59 (1973) 2902.

[16] S. Aridizzone, P. Siviglia, S. Trasatti, J. Electroanal. Chem. 122 (1981) 395.
[17] R.C. West (Ed.), CRC Handbook of Chemistry and Physics, 70th edn.,1989, p. E-117.
[18] D.T. Shieh, B.J. Hwang, J. Electroanal. Chem. 391 (1995) 77.
[19] E. Amouyal, P. Keller, A. Moradpour, J. Chem. Soc., Chem. Comm. (1980) 1019.
[20] J.M. Kleijn, G.K. Boschloo, J. Electroanal. Chem. 300 (1991) 595.
[21] A. Mills, N. McMurray, J. Chem. Soc., Faraday Trans. 1 84 (1988) 379.
[22] K.J. Takeichi, G.J. Samuels, S.W. Gerstein, J.A. Gilbert, T.J. Meyer, Inorg. Chem. 22 (1983) 1409.
[23] A. Mills, T. Russell, J. Chem. Soc., Faraday Trans. 87 (1991) 313.
[24] M. Yagi, K. Nagoshi, M. Kaneko, J. Phys. Chem. B 101 (1997) 5143.
[25] A.J. Bard, L.R. Faulkner, Electrochemical Methods, Fundamentals and Applications, Wiley, New York, 1980.
[26] C.R. Martin, I. Rublinstein, A.J. Bard, J. Am. Chem. Soc. 104 (1982) 4817.